Determination of heterojunction band offsets between CdS bulk and PbS quantum dots using photoelectron spectroscopy

Khagendra P. Bhandari,[1] Hyekyoung Choi,[2] Sohee Jeong,[2,3] Hasitha Mahabaduge,[1] and Randy J. Ellingson[1,a)]

[1]Department of Physics and Astronomy, The University of Toledo, 2801 W. Bancroft Street, Mail Stop 111, Toledo, Ohio 43606, USA
[2]Department of Nanomechatronics, Korea University of Science and Technology, Daejeon 305-350, South Korea
[3]Nanomechanical Research Division, Korea Institute of Machinery and Materials, Daejeon 305-343, South Korea

Photoelectron spectroscopy was used to measure the energy discontinuity in the valence band (ΔE_V) of a CdS/PbS quantum dot (QD) heterojunction for which the PbS QD layer was deposited using solution based layer-by-layer dip coating method on top of RF magnetron sputtered CdS. A value of $\Delta E_V = 1.73$ eV was obtained using the Cd 3d and Pb 4f energy levels as references. Given the band gap energies of the CdS and PbS-QD layers, the conduction band offset ΔE_C was determined to be 0.71 eV. © 2014 AIP Publishing LLC. [http://dx.doi.org/10.1063/1.4897301]

A heterojunction interface is formed at the boundary between two dissimilar semiconductors. In many cases, materials scientists seek to optimize heterojunction quality by minimizing the lattice mismatch across the junction. Valence band offsets have been very well studied in lattice matched heterojunctions.[1,2] Heterojunctions formed from materials exhibiting considerable lattice mismatch incorporate strain into one or both sides of the interface.[3,4] It has been pointed out that core level (CL) to valence band edge (VBE) binding energies depend on the strain arising from lattice mismatch.[5] In such strained interfaces, strain both shifts and splits the CL-to-VBE energies, and the actual valence and conduction band discontinuities depend on the details of the strain at and near the interface.[6] The conduction and valence band discontinuities ΔE_C and ΔE_V that occur at a heterojunction interface and depend on lattice mismatch and the abrupt band gap change (ΔE_g) can be used to improve the design of solid state electronic devices.[1,2,7] Accurate knowledge of an interface's valence band offset (ΔE_V) and the factors that influence its magnitude are thus of both fundamental and practical interest. In this paper, the CdS/PbS-quantum dot (QD) system is chosen for analysis for several reasons. First, it displays a relatively high room-temperature lattice mismatch ($\sim$11.6%) with CdS. This value was calculated by using lattice constant (a = 4.136 Å, c = 6.714 Å) of CdS,[8,9] and lattice constant (a = 5.936 Å) of PbS.[10] Second, to date there is no information available on the band offsets between bulk CdS and PbS-QD films.[11] Third, an accurate knowledge of the valence band offset ΔE_V and conduction band offset ΔE_C at the CdS/PbS-QD heterojunction interface owing to the band gap difference (ΔE_g) between hexagonal wurtzite CdS ($E_g = 2.42$ eV)[12] and rock salt PbS QD[13] is important for device design, modelling, and performance prediction. This paper discusses how photoelectron spectroscopy, including both ultraviolet photoemission spectroscopy (UPS) and x-ray photoelectron spectroscopy (XPS), can be applied to directly, contactlessly, and quantitatively measure the valence band offset at abrupt heterojunction interfaces within the CdS/PbS-QD system.

CdS growth was performed using RF magnetron sputtering, at a sputter power of 50 W, onto Pilkington TEC™ 15 SnO$_2$:F (transparent conducting oxide, TCO) coated soda lime glass. The thickness of the all sputtered CdS films was standard at $\sim$70 nm. To form the PbS-QD layers, we utilized 2.8 nm diameter colloidal PbS QDs ($E_g \approx 1.40$ eV), synthesized via thermal injection in an N$_2$ atmosphere Schlenk line.[14,15] The interface of CdS/PbS-QD heterojunction was prepared at room temperature by depositing PbS QD-based thin films of various thicknesses using a layer-by-layer (LbL) dip coating method in which the as-prepared oleic acid ligands are replaced with a short chain molecule, 1,2-ethanedithiol.[15–17] For UPS/XPS measurement, Au/CdS, TCO/CdS, TCO/PbS-QD, TCO/CdS/PbS-QD, and Au/CdS/PbS-QD films were prepared and then transferred into the UPS/XPS spectrometer. All spectra were collected at room temperature in an ultrahigh vacuum photoelectron spectrometer equipped with an electron energy analyzer (constant analyzer energy) with He-I radiation (hν = 21.22 eV) as UV source and Al Kα (hν = 1486.6 eV) anode operated at 150 W, as X-ray source.

The XPS CL spectra were acquired for the bulk CdS film and PbS-QD film, each deposited onto TEC 15 glass substrates. XPS and UPS studies were also done for CdS and PbS-QD films deposited on Au-coated glass substrates.[18] Core level spectra were acquired for seven different samples of PbS-QD films on CdS, each of which consisted of different QD film thicknesses ranging from $\sim$3 nm to $\sim$200 nm. Initially, CL survey scans were performed in order to determine elemental composition and their relative abundance. For most of the samples analyzed in this work, no peaks were present at energies higher than 800 eV. Very high resolution spectra were then acquired over narrow energy ranges in order to determine the binding energy of specific elements

a)Author to whom correspondence should be addressed. Electronic mail: Randy.Ellingson@utoledo.edu. Tel.: +001 419 530 3874.

105, 131604-1
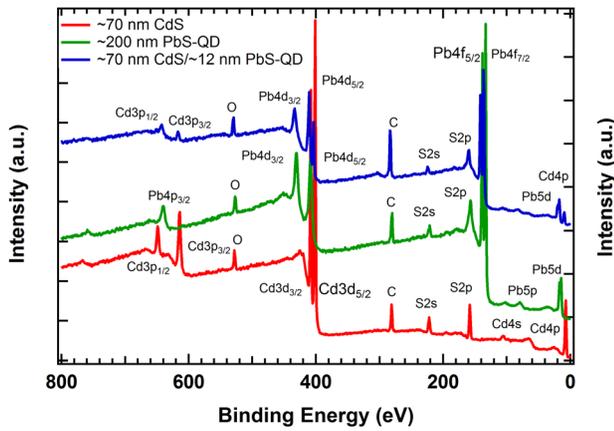
FIG. 1. Core level survey spectra of 70 nm layer of CdS, 200 nm PbS-QD, and 12 nm PbS-QD/70 nm CdS films, each deposited on NSG TEC 15 glass substrate.

observed in the survey spectra. Figure 1 shows XPS CL survey spectra for a 70 nm-thick CdS film, a 200 nm-thick PbS-QD film, and a 12 nm-thick PbS-QD film deposited onto 70 nm thick CdS.

Figure 2 shows CL spectra of Cd 3d and Pb 4f when the thickness of the PbS-QD film deposited onto CdS is varied from a single layer of QDs (monolayer, 3 nm) to 200 nm. There is an evident but comparatively small shift of the Cd 3d (toward larger BE) and Pb 4f (toward smaller BE) lines as the
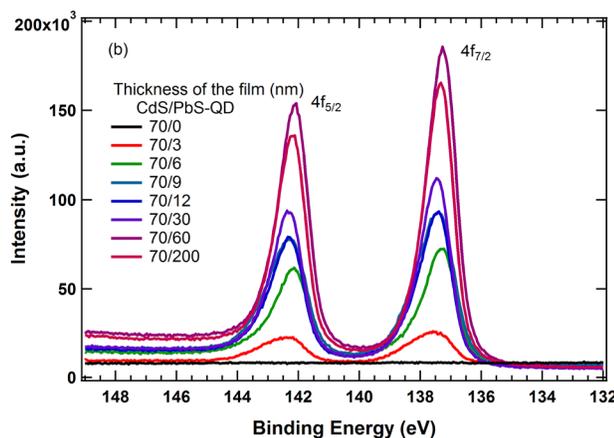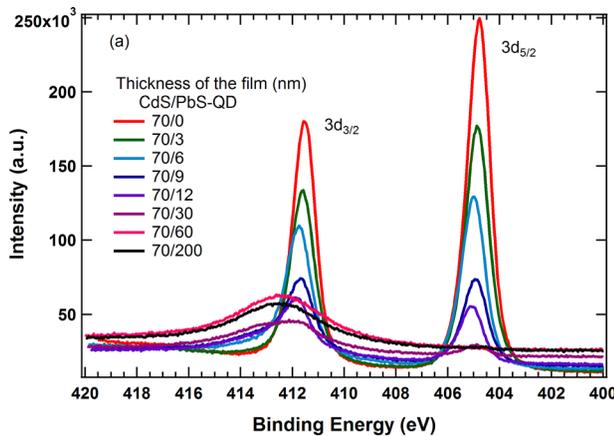
FIG. 2. Photoemission spectra of (a) Cd and (b) Pb CLs measured after each PbS-QD growth step on CdS substrate; broad peaks near 412.5 eV for PbS-QD layer thickness of 30, 60, and 200 nm are not attributed to the Cd $3d_{3/2}$ transition.

PbS-QD layer thickness increases, which may indicate the formation of a depletion region (band bending) in PbS-QD layer. As the thickness of PbS-QD layer increases, the Cd 3d emission gradually decreases in intensity to zero and the Pb 4f emission gradually increases in intensity to a maximum. For PbS-QD layer thicknesses ranging from 0 to 12 nm, the CL binding energies of Cd $3d_{3/2}$ and Cd $3d_{5/2}$ peaks shifted to higher binding energy by an average of 0.32 eV. Similarly, the CL binding energies of Pb $4f_{5/2}$ and Pb $4f_{7/2}$ peaks shifted to higher binding energies, by an average of 0.17 eV, when the thickness of PbS-QD layer was decreased from 200 nm to 12 nm. Thickness-dependent CL peak positions are provided in the supplementary material. These small shifts in binding energies are due to the similarity of carrier concentrations in CdS and PbS-QD (CdS: 9.95×10^{15} cm^{-3} vs PbS-QD $= 5.6 \times 10^{16}$ cm^{-3}).[15] Reaching the 60 nm PbS-QD layer thickness, the Cd 3d emission lines are completely suppressed, revealing an unidentified peak at ~412.5 eV (Figure 2). Sulfur is contained in both the CdS and the top PbS-QD layers; however, the S 2p spectra differ for CdS and PbS-QDs due to the organic thiol molecules present within the QD film (see supplementary material for detail).

A CL photoemission-based method was used to determine the valence band offset.[1,19–21] Appropriate CL peaks were referenced to the top of the valence band for the CdS and PbS QD, where the top of the valence band (VBM, E_v) was determined using a linear extrapolation of the leading edge of valence band in UPS spectra.[15] Referring to the CdS/PbS-QD band diagram shown in Figure 3, ΔE_v can be determined from the change in differential binding energy between CLs from each side of the interface as given by

$$\Delta E_v = \Delta E_{CL} + (E_{Pb4f}^{PbS} - E_v^{PbS}) - (E_{Cd3d}^{CdS} - E_v^{CdS}), \quad (1)$$

where ΔE_{CL} is the binding energy difference between the CLs as measured for the interfaced CdS and PbS-QDs, $\Delta E_{CL} = (E_{Cd3d}^{CdS} - E_{Pb4f}^{PbS})$. Core level peak positions were located with Gaussian curve fits to the XPS spectra by a fitting procedure using IGOR Pro software.

Figure 3 incorporates data acquired by both UPS and XPS methods. In this case, UPS provides a more precise
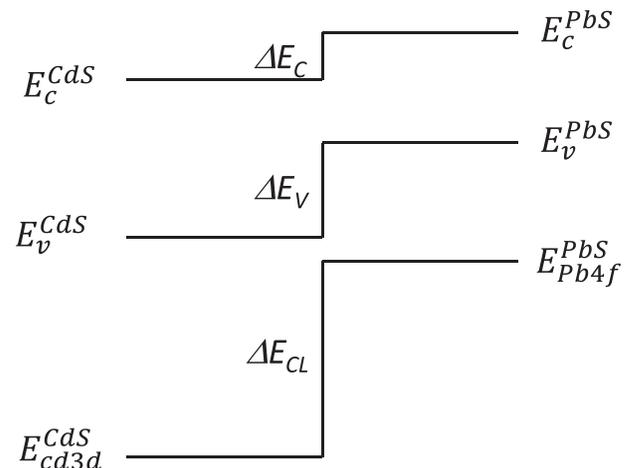
FIG. 3. The schematic band diagram of the interface between CdS and PbS QDs. The referenced Cd 3d and Pb 4f CLs of CdS and PbS QDs are also indicated qualitatively.

value for the valence band maxima for both PbS-QD and CdS layers in their non-interacting forms. However, UPS does not allow for measurement of CLs necessary to determine the valence band offset in interacting (interfaced) layers.

XPS spectra for both CdS and PbS-QD films are presented in Figure 4; these spectra show the Cd 3d CL peaks from the CdS layer and the Pb 4f CL peaks from PbS-QD layer. Figure 4(a) provides Cd 3d and Pb 4f spectra before the heterojunction is formed. In this case, Cd has two significant spectral lines, namely, Cd $3d_{3/2}$ at 411.54 ± 0.05 eV and Cd $3d_{5/2}$ at 404.81 ± 0.05 eV; Pb has also two significant spectral lines, namely, Pb $4f_{5/2}$ at 142.16 ± 0.05 eV and Pb $4f_{7/2}$ at 137.3 ± 0.05 eV, respectively. The doublets arise from spin-orbit splitting which occurs for p, d, and f CLs. The spin-orbit separation (Δ) for the Cd 3d lines is 6.73 ± 0.05 eV and for the Pb 4f lines is 4.86 ± 0.05 eV. The XPS spectra for the S 2p and O 1s CLs are provided in Figure S1, along with a detailed analysis of each binding energy peak for s, p, d, and f levels. Figure 4(b) shows Cd 3d and Pb 4f CL binding energy spectra after the heterojunction is formed between CdS and PbS-QD layers. These spectra are used to calculate the CL binding energy difference between the two materials.

In Figure 4(b), A and B denote the CL energy difference (ΔE_{CL}) between Cd 3d and Pb 4f states at the heterojunction.
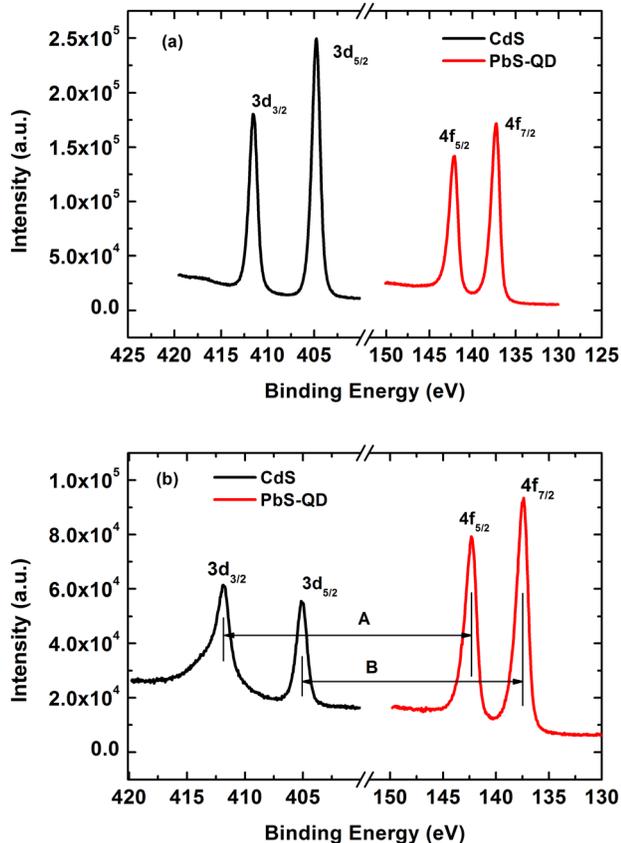
FIG. 4. (a) XPS binding energy spectra of CdS-bulk and PbS-QD films, each deposited onto NSG TEC 15 coated glass substrates. (b) XPS binding energy spectrum of PbS-QD/CdS-bulk heterojunction sample in the region of the Pb 4f and Cd 3d CLs and when the PbS-QD layer thickness is ~12 nm. A and B represent the binding energy difference between the CLs of Cd and Pb.
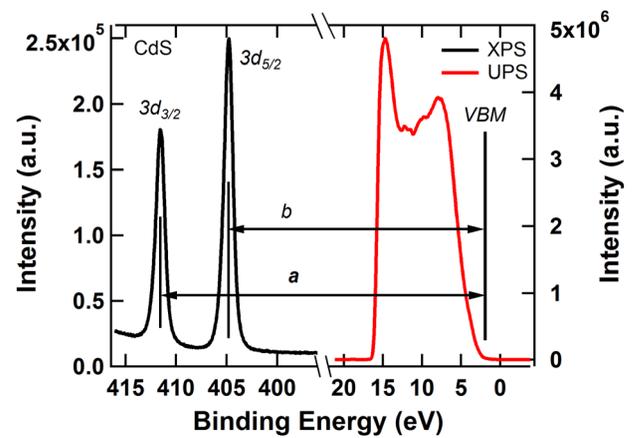
FIG. 5. XPS and UPS binding energy spectra for CdS. Letters "*a*" and "*b*" represent the binding energy difference between Cd 3d CL and the CdS VBM.

The value of A and B are calculated to be 269.56 ± 0.05 eV and 267.63 ± 0.05 eV, respectively. The valence band maximum E_v was obtained from the UPS spectra shown in Figures 5 and 6 by linearly fitting the leading edge of the valence band and extrapolating the fitted line to the x-axis. We found E_V for CdS resides 2.00 ± 0.10 eV below the Fermi level, which lies within the range of previously reported values.[22–24] As the band gap of CdS is at 2.42 eV, the Fermi level is 0.42 eV below the conduction band level (note that the spacing between the CdS conduction band and Fermi level and that between the PbS-QD VB and Fermi level are coincidentally both 0.42 eV for this size PbS QD). The Fermi level positions make sense since for n-type CdS, the Fermi level is expected to reside closer to the conduction band. We found the VBM of the PbS-QD layer resides at ~0.42 eV ± 0.10 from the Fermi level. Given the optical gap of $E_g \approx 1.40$ eV for these QDs, and that the PbS-QD layer is p-type, the Fermi level lies, as expected, close to the valence band edge.

The second and third terms in Eq. (1) can be calculated with the help of Figures 5 and 6. In Figure 5, the difference between Cd $3d_{3/2}$ and VBM is denoted by "*a*" and Cd $3d_{5/2}$ and VBM is denoted by "*b*;" "*a*" and "*b*" are determined to be 409.54 ± 0.1 eV and 402.81 ± 0.1 eV, respectively.
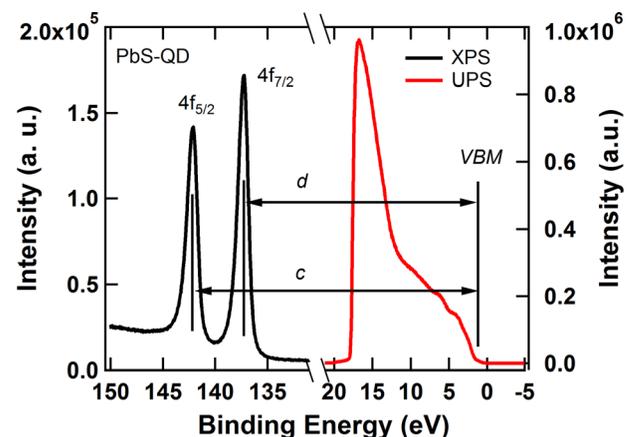
FIG. 6. XPS and UPS binding energy spectra for PbS-QD. Letters "*c*" and "*d*" denote the binding energy difference between Pb 4f CL and the VBM.

TABLE I. Calculated parameters to satisfy Eq. (1).

Core Level	ΔE_{CL} (eV)	$(E_{Pb4f}^{PbS} - E_v^{PbS})$ (eV)	$(E_{Cd3d}^{CdS} - E_v^{CdS})$ (eV)	Valence band offset (eV)
$Cd3d_{5/2}\&Pb4f_{7/2}$	269.56 ± 0.05	141.74 ± 0.1	409.54 ± 0.1	1.76 ± 0.10
$Cd3d_{3/2}\&Pb4f_{5/2}$	267.63 ± 0.05	136.88 ± 0.1	402.81 ± 0.1	1.70 ± 0.10

In Figure 6, the difference between Pb $4f_{5/2}$ and the PbS-QD VBM is denoted by "*c*" and Pb $4f_{7/2}$ and the VBM is denoted by "*d*." Substituting the values, "*c*" and "*d*" are determined to be 141.74 ± 0.1 eV and 136.88 ± 0.1 eV, respectively.

Now, we have all required information to calculate valence band offset ΔE_v in Eq. (1). For convenience, these values are collected in Table I.

The average value of the valence band offset was calculated to be 1.73 ± 0.10 eV. Given the band gap of CdS is 2.42 eV and PbS QDs is 1.40 eV, the conduction band offset, ΔE_c, is calculated to be 0.71 ± 0.10 eV.

Figure 7 shows the schematic of the energy band lineup in the CdS/PbS-QD heterojunction, with all of the energy scales included. The indicated type II heterojunction aids in charge separation across the interface, with electrons tending to transfer toward the CdS and holes toward the PbS-QD layer.

We have determined the valence band offset in CdS/PbS-QD heterojunction samples. For this heterojunction system, our measurements yield a valence band offset of 1.73 eV and a conduction band offset of 0.71 eV. These values are compatible with reasonably efficient electron injection from the PbS-QDs into CdS, supporting the continuing study of QD-based electro-optical applications such as photovoltaic devices. This quantitative study contributes to the understanding of the energetics of interfaces between bulk and nanostructured semiconductors.

[1]J. R. Waldrop, R. W. Grant, S. P. Kowalczyk, and E. A. Kraut, J. Vac. Sci. Technol., A **3**(3), 835 (1985).
[2]E. T. Yu, D. H. Chow, and T. C. McGill, J. Vac. Sci. Technol., B **7**(2), 391 (1989).
[3]G. Liu, T. Schulmeyer, J. Brötz, A. Klein, and W. Jaegermann, Thin Solid Films **431–432**(0), 477 (2003).
[4]E. A. Douglas, A. Scheurmann, R. P. Davies, B. P. Gila, H. Cho, V. Craciun, E. S. Lambers, S. J. Pearton, and F. Ren, Appl. Phys. Lett. **98**(24), 242110 (2011).
[5]J. Tersoff and C. G. Van de Walle, Phys. Rev. Lett. **59**(8), 946 (1987).
[6]G. P. Schwartz, M. S. Hybertsen, J. Bevk, R. G. Nuzzo, J. P. Mannaerts, and G. J. Gualtieri, Phys. Rev. B **39**(2), 1235 (1989).
[7]E. T. Yu, E. T. Croke, D. H. Chow, D. A. Collins, M. C. Phillips, T. C. McGill, J. O. McCaldin, and R. H. Miles, J. Vac. Sci. Technol., B **8**(4), 908 (1990).
[8]N. G. Stoffel, Phys. Rev. B **28**(6), 3306 (1983).
[9]O. Madelung, *Semiconductors: Other Than Group IV Elements and III-V Compounds* (Springer-Verlag, 1992), p. 164.
[10]I. Moreels, K. Lambert, D. Smeets, D. De Muynck, T. Nollet, J. C. Martins, F. Vanhaecke, A. Vantomme, C. Delerue, G. Allan, and Z. Hens, ACS Nano **3**(10), 3023 (2009).
[11]B. A. Timp and X. Y. Zhu, Surf. Sci. **604**(17–18), 1335 (2010).
[12]Y. H. Sun, Y. J. Ge, W. W. Li, D. J. Huang, F. Chen, L. Y. Shang, P. X. Yang, and J. H. Chu, J. Phys.: Conf. Ser **276**(1), 012187 (2011).
[13]I. Kang and F. W. Wise, J. Opt. Soc. Am. B **14**(7), 1632 (1997).
[14]J. M. Luther, J. Gao, M. T. Lloyd, O. E. Semonin, M. C. Beard, and A. J. Nozik, Adv. Mater. **22**(33), 3704 (2010).
[15]K. P. Bhandari, P. J. Roland, H. Mahabaduge, N. O. Haugen, C. R. Grice, S. Jeong, T. Dykstra, J. Gao, and R. J. Ellingson, Sol. Energy Mater. Sol. Cells **117**(0), 476 (2013).
[16]K. P. Bhandari, H. Mahabaduge, J. Gao, and R. J. Ellingson, Proc. SPIE **8824**, 88240I (2013).
[17]J. M. Luther, M. Law, M. C. Beard, Q. Song, M. O. Reese, R. J. Ellingson, and A. J. Nozik, Nano Lett. **8**(10), 3488 (2008).
[18]See supplementary material at http://dx.doi.org/10.1063/1.4897301 for elemental analysis of CdS and PbS films using XPS.
[19]E. A. Kraut, R. W. Grant, J. R. Waldrop, and S. P. Kowalczyk, Phys. Rev. B **28**(4), 1965 (1983).
[20]J. R. Waldrop and R. W. Grant, Appl. Phys. Lett. **68**(20), 2879 (1996).
[21]R. W. Meulenberg, J. R. I. Lee, A. Wolcott, J. Z. Zhang, L. J. Terminello, and T. van Buuren, ACS Nano **3**(2), 325 (2009).
[22]A. Klein, C. Körber, A. Wachau, F. Säuberlich, Y. Gassenbauer, S. P. Harvey, D. E. Proffit, and T. O. Mason, Materials **3**(11), 4892 (2010).
[23]A. Santoni, F. Biccari, C. Malerba, M. Valentini, R. Chierchia, and A. Mittiga, J. Phys. D: Appl. Phys. **46**(17), 175101 (2013).
[24]K. Ellmer, A. Klein, and B. Rech, *Transparent Conductive Zinc Oxide: Basics And Applications In Thin Film Solar Cells Series* (Springer, Berlin, 2008).

FIG. 7. Energy band diagram of CdS/PbS-QD heterojunction interface. All parameters as obtained from the measurement are labeled and expressed in eV.